Nano Research

Open Access

Review Article

Atom-precise construction of fully conjugated curved carbon nanostructures

Qirui Long[1], Ming-Wei Wang[1], Wei Jiang[2], and Zhaohui Wang[1] ✉

[1] *Key Laboratory of Organic Optoelectronics and Molecular Engineering, Department of Chemistry, Tsinghua University, Beijing 100084, China*
[2] *School of Chemical Sciences, University of Chinese Academy of Sciences, Beijing 100049, China*

Cite this article: *Nano Research*, **2026**, *19*, 94908735. https://doi.org/10.26599/NR.2026.94908735

ABSTRACT: Atomically precise carbon nanomaterials with curved topologies define a central direction in modern synthetic chemistry and materials science. Motivated by the pioneering discovery of fullerenes, this pursuit has evolved to encompass the precision synthesis of carbon allotropes across dimensionalities, from zero-dimensional fullerenes and quasi-one-dimensional carbon nanotubes to three-dimensional schwarzites. This review summarized recent progress in bottom-up strategies towards these targets, highlighting the rational synthesis of key molecular segments. It formulated how such structurally defined fragments serve as both fundamental building blocks and critical model systems. These advances have not only enabled the establishment of precise structure–property relationships but also opened pathways for their controllable assembly. How to transform these discrete molecular units into macroscopically ordered and extended architectures, such as schwarzites, still remains great challenge.

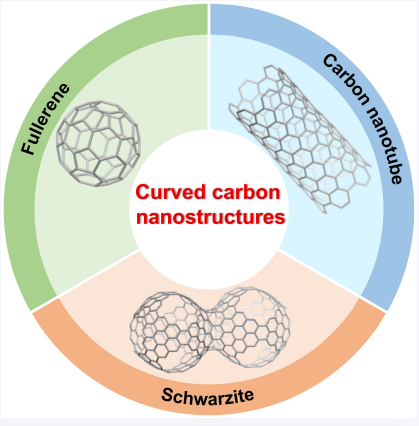

KEYWORDS: curved carbon nanostructures, fullerenes, molecular carbons, schwarzite carbons, polycyclic aromatic hydrocarbons

1 Introduction

Recent decades have witnessed the exploration of numerous novel curved carbon allotropes, driven by advances in synthesis and characterization techniques. The spherical carbon allotrope C_{60}, commonly known as fullerene, was first identified by Kroto and colleagues in 1985 through laser ablation experiments [1]. Subsequently, Iijima reported the discovery of carbon nanotubes (CNTs) during arc-discharge evaporation [2]. Building on these experimental advances, in 1991, Mackay proposed a new form of three-dimensional (3D) curved carbon allotrope, now referred to as schwarzite, by theoretically decorating the triply periodic minimal surface (TPMS) with sp^2-hybridized carbon atoms [3]. The special topological structures endow these fully conjugated curved carbon allotropes with intriguing physicochemical properties, offering potential applications in electronic devices and advanced engineering materials.

Received: January 1, 2026; **Revised:** April 10, 2026
Accepted: April 14, 2026

✉Address correspondence to wangzhaohui@mail.tsinghua.edu.cn

The topological characteristics of these fully conjugated curved structures can be quantitatively described using Gaussian curvature (K), defined at a point on a surface as the product of the two principal curvatures, k_1 and k_2, representing the maximum and minimum curvatures of all curves passing through the given point, respectively. Fullerenes, possessing spherical topology, exhibit positive Gaussian curvature ($K > 0$) across their entire surface. Carbon nanotubes, with cylindrical topology, demonstrate zero Gaussian curvature (Fig. 1). Conversely, schwarzite, defined by a triply periodic minimal surface structure, displays a negative Gaussian curvature ($K < 0$) [3, 4]. These curved carbon nanomaterials exhibit distinctive electronic properties arising from their characteristic curvatures, establishing them as a major focus in materials science and nanotechnology [5–10].

Although conjugated carbon nanomaterials with complex topologies have been analyzed and characterized using techniques such as scanning electron microscopy and spectroscopy, achieving their macroscale synthesis with atomic precision remains a formidable challenge. Traditional material synthesis methods, such as electric arc techniques and laser irradiation, have achieved considerable success in producing closed-cage molecules like C_{60} [11, 12]. Arc-discharge, laser ablation, and chemical vapor deposition (CVD) have made significant progress in industrial-scale

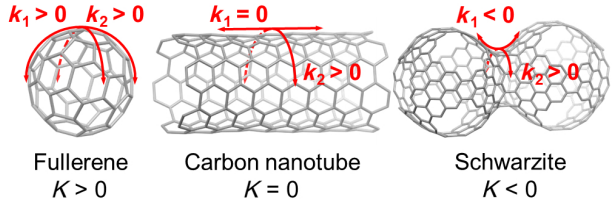

Figure 1 Curved carbon nanostructures.

production of carbon nanotubes, but still face considerable challenges in achieving precise control over edge structures and length. Moreover, such methods often generate substantial amounts of amorphous carbon, metal catalyst particles, and various other impurities, while simultaneously producing carbon nanomaterials with diverse sizes and fine structures. These complex mixtures pose significant challenges for the separation and purification of conjugated carbon nanomaterials. In particular, trace impurities that are difficult to remove hinder in-depth investigations of the intrinsic properties of this class of conjugated carbon nanomaterials.

Besides the aforementioned methods, the bottom-up strategy has become increasingly important in the synthesis of curved carbon nanomaterials. Molecular carbons are defined as a class of structurally precise and monodisperse nanocarbon architectures that serve as critical models for deciphering structure–property relationships in carbon-based nanomaterials. As the synthetic methodology has progressed by leaps and bounds, the cross-coupling reactions catalyzed by transition metals facilitate the interconnections of two carbon moieties, such as the Suzuki cross-coupling, Negishi cross-coupling, and Heck cross-coupling reactions. This bottom-up approach not only facilitates the creation of complex carbon nanostructures with intriguing properties but also provides a fundamental platform for exploring physical and chemical properties in nanoscale carbon systems. This review summarized recent advances in the synthesis of curved molecular carbons with different topological structures aiming to stimulate the precise synthesis of novel carbon nanostructures.

2 Carbon nanostructures with positive curvature

In 1985, Kroto et al. simulated the high vacuum and high-energy conditions of cosmic nebulae [1]. They introduced pure graphite into this high vacuum environment and irradiated it with a high-power laser. They observed the formation of C_{60} in mass spectrometry. They proposed that its structure was a perfect hollow soccer ball-shaped sphere composed of 12 pentagons and 20 hexagons, naming it Buckminsterfullerene (commonly referred to as fullerene or Buckyball). Subsequently, in 1990, Krätschmer et al. successfully produced single crystals of C_{60} via arc discharge [11] and unambiguously confirmed the soccer ball-like structure of C_{60} via X-ray diffraction.

The discovery of C_{60} not only unveiled the existence of fullerene materials but also represented a major breakthrough in atomically precise carbon nanomaterials. According to Euler's theorem, classical fullerenes consist of closed cage structures formed by 12 pentagonal rings and a variable number of hexagonal rings, with the total number of carbon atoms following the mathematical relationship $n = 20 + 2i$ (where i denotes the number of hexagons) [13]. As the most representative member of this series, C_{60} is composed of 12 pentagons and 20 hexagons arranged in a spherical configuration. Its hollow cage structure, with an outer diameter of approximately 0.71 nm, could be considered as a zero-dimensional carbon nanomaterial. C_{60} and its derivatives exhibit remarkable potential in multidisciplinary applications owing to their unique electronic configuration and structural adaptability. They could function as core components in organic photovoltaic devices by facilitating charge separation and transport [14], neuroprotective agents [15], hosts for drug delivery systems [16], and catalysts in synthetic transformations [17, 18]. These applications demonstrate C_{60}'s versatility as a multifunctional nanomaterial with tailored properties for advanced technologies.

Although C_{60} and C_{70} can be synthesized on an industrial scale through arc discharge and combustion methods currently, continued interest in the unique properties of its curved cage structure has motivated several research groups to pursue bottom-up approaches for the precise organic synthesis of C_{60}. Early theoretical work suggested that precursor **1** might spontaneously rearrange into C_{60} in the gas phase via a 60-carbon ring cyclo[60]carbon intermediate (Fig. 2(a)) [19]. Due to the synthetic challenges associated with producing such a large ring system, Rubin and colleagues proposed an alternative strategy using carbon

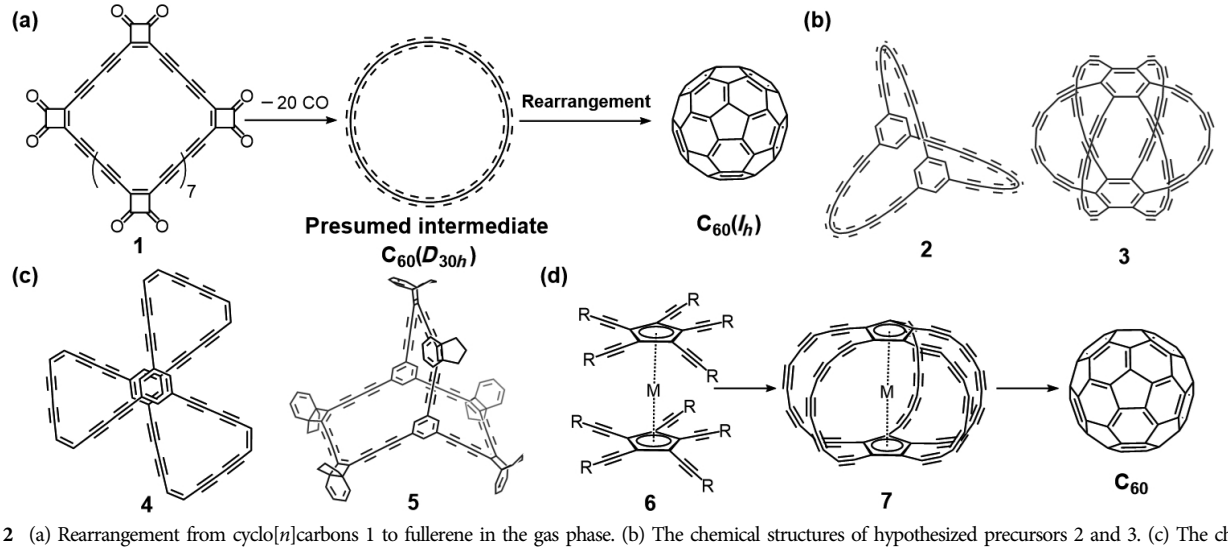

Figure 2 (a) Rearrangement from cyclo[*n*]carbons 1 to fullerene in the gas phase. (b) The chemical structures of hypothesized precursors 2 and 3. (c) The chemical structures of synthesized precursors 4 and 5. (d) Rearrangement from hypothesized metallocene precursors 6 and 7 to fullerene.

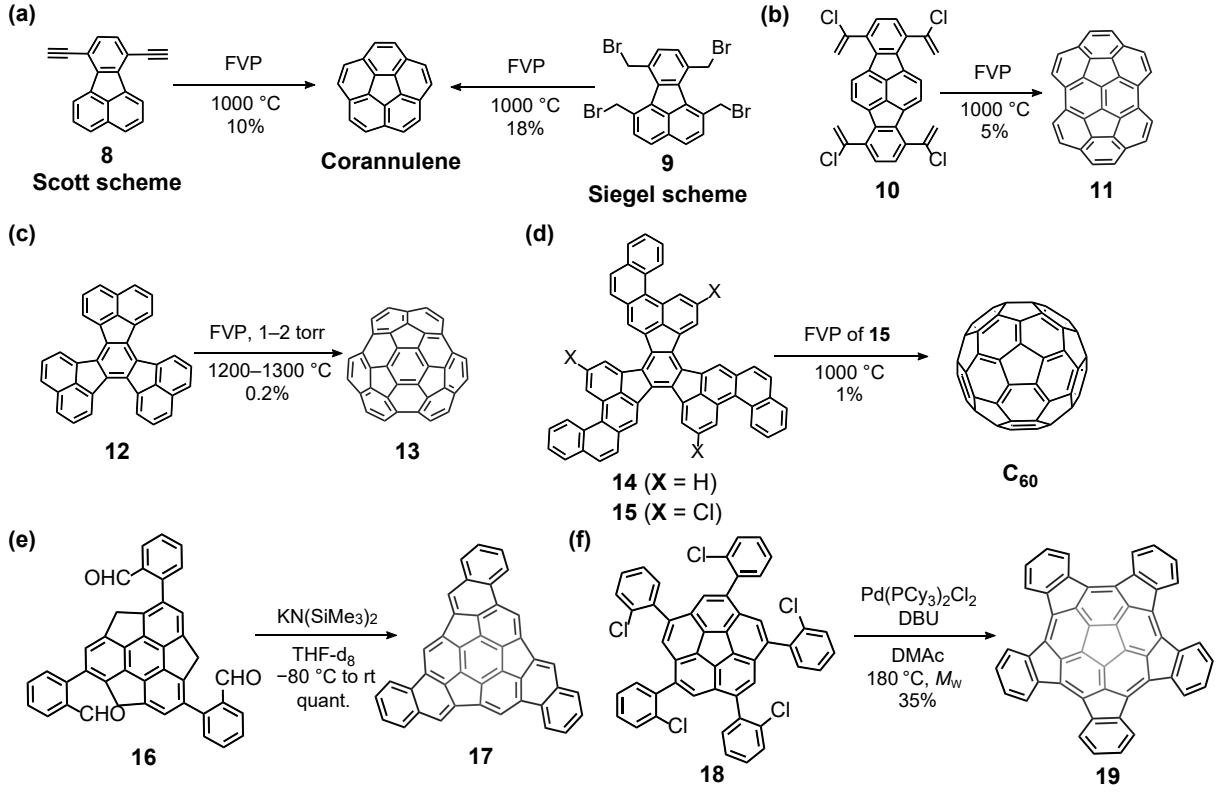

Figure 3 (a) Synthesis of corannulene using FVP. (b) Synthesis of segment 11 by using FVP. (c) Synthesis of segment 13 by using FVP. (d) Synthesis of C_{60} by using FVP. (e) Synthesis of segment 17 from a trisubstituted sumanene 16. rt: room temperature. (f) Synthesis of a pentaindenocorranulene 19.

cage precursors **2** and **3**, which could potentially undergo dehydrogenation or rearrangement to form fullerenes (Fig. 2(b)) [20]. They successfully synthesized precursor **4**, but mass spectrometry results revealed lower mass peaks *m*/*z* from 734 to 737, indicating that the precursor undergoes dehydrogenation at least down to $C_{60}H_{14}$, with no evidence of fullerene formation. In a separate effort, Tobe et al. synthesized an adduct of **2** and indane (precursor **5**) and observed the generation of fullerene ions via laser desorption mass spectrometry (Fig. 2(c)) [21]. Nevertheless, the yield was too low to permit isolation. In addition to the aforementioned approaches using benzene rings as the core structure for carbon cage formation, Bunz et al. investigated a synthetic strategy employing **7** as precursors (Fig. 2(d)) [22]. However, due to the challenging synthesis of the precursor complexes, this method failed to succeed.

Another approach for the rational synthesis of C_{60} involves using polycyclic aromatic hydrocarbon (PAH) precursors, where pentagons are surrounded by hexagons, to form the fullerene cage via intramolecular C–C bond formation under high-temperature pyrolytic conditions. In 1991 and 1992, the research groups of Scott and Siegel independently reported simplified synthetic routes to corannulene using the flash vacuum pyrolysis (FVP) method, thereby introducing FVP as a viable technique for synthesizing "buckybowls" or "fullerene fragments" (Fig. 3(a)) [23, 24]. In 1994, Rabideau's team synthesized a semibuckminsterfullerene molecule via FVP, a structure containing 30 carbon atoms that maps directly onto the surface of C_{60} (Fig. 3(b)) [25]. Scott et al. and Rabideau et al. subsequently expanded this methodology significantly [26–29]. The following year, Rabideau et al. reported another FVP-derived molecule, hemifullerene, centered on a six-membered ring framework [30]. In 1996, Scott et al. synthesized a larger fullerene fragment **13**, whose configuration closely resembles that of C_{60} (Fig. 3(c)) [31]. 2001, his group reported a $C_{60}H_{30}$ PAH (structure **14**), whose Schlegel diagram revealed that it already contained 13 of the 20 benzene rings and 75 of the 90 C–C bonds required to form C_{60} [32]. Although mass spectrometry indicated that this precursor could undergo "stitching" under high-energy laser irradiation, the isolation of pristine C_{60} remained unsuccessful. A breakthrough came in the next year, when Scott's group described an FVP procedure starting from a chlorinated hydrocarbon precursor **15** (Fig. 3(d)) [33]. This method achieved the formation of C_{60} with a yield of about 1%, marking the first targeted synthesis of the fullerene via a rational precursor route. Meanwhile, substantial progress has also been achieved through wet-chemical approaches [34]. In 2009, Hirao and co-workers used a trisubstituted sumanene **16** to obtain the deepened bowl **17** via triple Knoevenagel-like benzannulation (Fig. 3(e)) [35]. Scott et al. also obtained a pentaindenocorranulene **19** from a pentaaryl precursor **18** using catalytic direct arylation (Fig. 3(f)) [36].

In the synthetic routes involving polycyclic aromatic hydrocarbons (PAHs) described above, it has been elucidated that planar compounds containing benzene rings exhibit excellent compatibility with metal surfaces. This characteristic makes them highly suitable for applications such as surface-assisted cyclization, metal-catalyzed coupling reactions, or the formation of well-ordered self-assembled monolayers on metallic substrates. The planar geometry and extended π-system of these benzene-ring-containing compounds facilitate strong adsorption and electronic interaction with metal surfaces, which is crucial for achieving high efficiency and selectivity in related synthetic processes. Many of the carbon–carbon bond formation reactions between such aromatic systems are catalyzed by transition metals, including

Suzuki–Miyaura coupling, Ullmann coupling between two aryl halides, and even dehydrogenative coupling between two C–H bonds. This provides a theoretical foundation for the metal-catalyzed closure of fullerenes. In 2008, the first synthesis of C_{60} on a metal surface was achieved by Otero et al. (Fig. 4) [37]. They chose **20** as a precursor. Using scanning tunneling microscopy (STM) to monitor the chemical transformation process, they observed that when $C_{60}H_{30}$ was adsorbed on a Pt(111) surface, the three "wings" of the molecule were clearly visible, appearing as triangular features approximately 2.2 nm in length and 0.14 nm in height. After annealing at 750 K, all these triangular structures transformed into circular features with a reduced diameter of about 1.5 nm and an increased height of 0.38 nm. The reaction proceeded with nearly 100% yield. Furthermore, azafullerene $C_{57}N_3$ from **21** was synthesized with this method.

3 Carbon nanostructures with zero curvature

In 1991, Iijima accidentally produced multi-walled carbon nanotubes while preparing fullerenes using the arc discharge method [2]. Two years later, Iijima and Ichihashi, and Beyers et al. reported that single-walled carbon nanotubes could be synthesized via the arc discharge method with iron as a catalyst [38, 39]. Carbon nanotubes are a quasi-one-dimensional carbon allotrope with nanoscale diameters and macroscale lengths. They can be conceptualized as seamless and hollow tubular molecules formed by rolling single or multiple layers of graphene sheets in a specific direction and connecting them end to end. The carbon atoms are primarily bonded through sp^2 hybridization, forming a highly delocalized π-electron conjugated system. The rolling direction is determined by the chiral vector $\mathbf{C_h}$: $\mathbf{C_h} = n\mathbf{a_1} + m\mathbf{a_2}$, where ($n$, m) is a pair of integers known as the chiral indices, which uniquely define the electronic properties and geometric structure of the carbon nanotube [40]. When m = 0, it is referred to as zigzag-type, exhibiting semiconductor electronic properties; when $n = m$, it is called armchair-type, displaying metallic electronic properties; and when $n \neq m$ and $m \neq 0$, it is termed chiral-type or helical-type, most of which are semiconductors. The diameter can be directly calculated from the chiral indices (n, m). Therefore, the precise synthesis of carbon nanotubes with a single chirality is of great importance. Carbon nanotubes demonstrate exceptional versatility in advanced applications due to their extraordinary mechanical strength, tunable electronic properties, and high surface-to-volume ratio. In materials engineering, they serve as reinforcing agents in high-performance composites and flexible electronics [41]. Their unique electronic characteristics enable applications in nanoelectronics as transistors and interconnects [42]. Additionally, CNTs function as efficient catalyst supports in energy conversion systems and as robust scaffolds in biomedical devices for drug delivery and tissue engineering. These multifunctional capabilities position CNTs as pivotal nanomaterials for technological innovation across disciplines [43].

Metal-catalyzed chemical vapor deposition (CVD) has made overwhelming progress in the synthesis of carbon nanotubes with uniform chirality [44]. In 2003, Resasco and colleagues reported the enriched growth of (6, 5)/(7, 5) chirality-enriched single-wall carbon nanotubes (SWCNTs) using a bimetallic Co/Mo catalyst [45]. In 2005, Iijima et al. demonstrated an epitaxial relationship

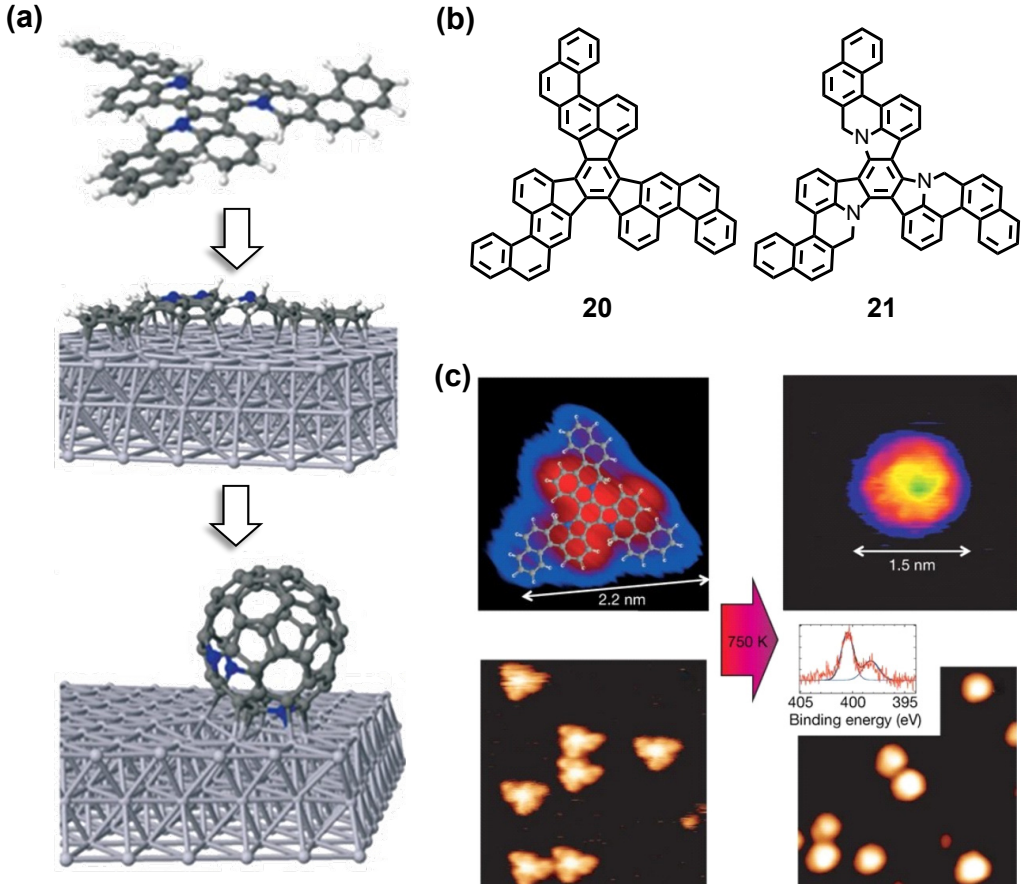

Figure 4 Synthesis of C_{60} on a Pt(111) surface. Reproduced with permission from Ref. [37], © Macmillan Publishers Limited 2008.

between cobalt nanocrystals and the growth of single-wall carbon nanotubes [46]. In 2006, Robertson et al. proposed for the first time an epitaxial growth model, predicting selective growth of single-wall carbon nanotubes on solid catalysts and suggesting that epitaxial growth on solid Ni catalysts could lead to chirality selectivity [47]. Subsequently, the principle of epitaxy was widely utilized to rationalize the chirality-controlled growth of SWCNTs [48, 49]. In 2014, Li et al. developed a bimetallic Co_7W_6 catalyst with a very high melting point and a rhombohedral crystal structure, achieving chirality-specific growth of single-wall carbon nanotubes, such as (12, 6), (16, 0), and (14, 4) [50–53].

Although carbon nanotubes produced via the CVD method currently dominate the market and meet the demands of numerous applications, their inability to precisely control length and edge structure remains an unresolved issue. Consequently, the bottom-up synthesis of single-walled carbon nanotubes continues to hold significant research importance. Following the successful precise synthesis of C_{60} using the FVP method, Scott and his team also attempted to apply this approach to the precise synthesis of carbon nanotubes, ultimately achieving the synthesis of a (5, 5) CNT end-cap (Fig. 5(a)) [54]. This molecule features an armchair-type edge structure, offering potential for subsequent tubular structure synthesis through Diels–Alder reactions, or as seeds for carbon nanotube growth. Another bottom-up synthesis route utilizes cyclopara-phenylenes (CPPs) as the starting material, which can be regarded as the simplest segments of armchair carbon nanotubes. In 2013, Itami and his team utilized CPP as a template to grow uncapped sidewall segments of carbon nanotubes (Fig. 5(b)) [55]. In 2014, Amsharov, Fasel, and their colleagues synthesized an ultra-short singly capped (6, 6) SWCNT through surface-catalyzed cyclodehydrogenation (Fig. 5(c)) [56]. They further reported using this structure as a seed for the epitaxial growth of SWCNTs exceeding 300 nm in length. In 2015, Zhou et al. pioneered a novel approach for the metal-free catalysis of nearly pure SWCNTs from molecular seeds [57].

Therefore, the precise synthesis of well-defined CPPs can be regarded as a crucial preliminary research objective. In 2008, Jasti et al. first proposed a synthetic approach in which a macrocyclic precursor was obtained via Suzuki coupling, followed by reduction using lithium naphthalenide to produce [9]-, [12]-, and [18]CPP (Fig. 6(a)) [58]. One year later, Itami and colleagues reported a strategy for synthesizing [12]CPP through aromatization of a macrocyclic precursor (Fig. 6(b)) [59]. Another year later, Yamago et al. introduced an alternative route using a 4,4'-bis(trimethylstannyl)biphenyl **31** as the substrate, which was transformed into the target molecule [8]CPP via a cyclic platinum complex intermediate, followed by bromine-induced reductive elimination (Fig. 6(c)) [60]. In 2020, Tsuchido and coworkers employed a strategy and developed an efficient synthesis of [6]CPP using a cyclic digold(I) complex intermediate [61].

Carbon nanobelts (CNBs) are belt-shaped molecular carbons entirely composed of fused benzene rings. They possess at least a double-stranded structure, meaning that breaking at least two carbon–carbon bonds is required to fully unfold them into a planar configuration. The synthesis of such compounds has been a highly challenging scientific problem over the past few decades [62]. As early as 1991, Vögtle and colleagues reported attempts to synthesize these carbon nanobelts (Fig. 7(a)) [63]. The Vögtle belt can be conceptually described as a segment of an armchair carbon nanotube composed of two rows of structural units, or alternatively, as a macrocyclic nanobelt formed by connecting naphthalene units at their 1,8- and 4,5-positions. This fused nature results in significantly higher ring strain, making their synthesis considerably more challenging. In early efforts, Iyoda et al. observed a mass spectral signal corresponding to [10]cyclophenacene using laser desorption time-of-flight (LD-TOF) mass spectrometry (Fig. 7(b)) [64]. However, it was not until 2017 that the Itami's group achieved the first total synthesis of [12]CNB **39** via a strategy involving Wittig reaction to construct a precursor followed by a nickel(0) Yamamoto coupling to effect macrocyclization (Fig. 7(c)) [65]. One year later, they also synthesized [16]CNB and [24]CNB [66]. In 2019, Miao and colleagues reported a "ring-to-belt" approach for the synthesis of an armchair CNB **41** from a [12]CPP derivative [67]. The chiral CNB **43**, which represents a sidewall segment of chiral (18, 12)CNT, was also reported. They started from a [12]CPP derivative bearing twelve aryl substituents and performed a Scholl reaction to induce cyclodehydrogenation. The isopropoxy groups attached to the precursor not only improved solubility but also helped lower the oxidation potential through electron-donating

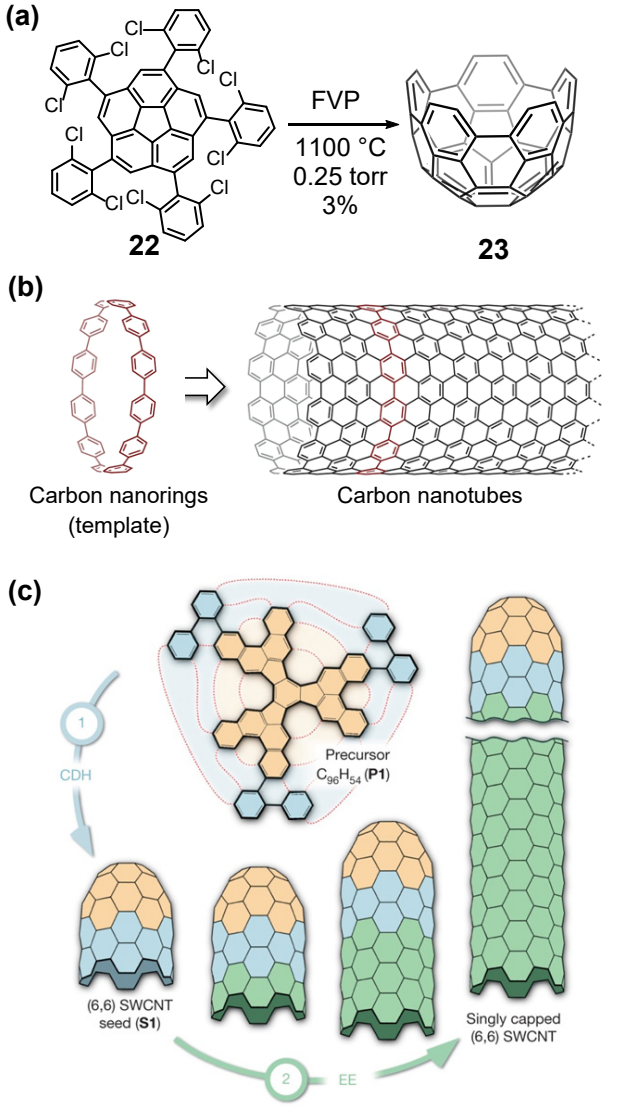

Figure 5 (a) Synthesis of a (5,5) CNT end-cap. ((b) and (c)) Synthesis of CNTs from its segments. Reproduced with permission from Ref. [55], © Springer Nature Limited 2013; Ref. [56], © Springer Nature Limited 2014.

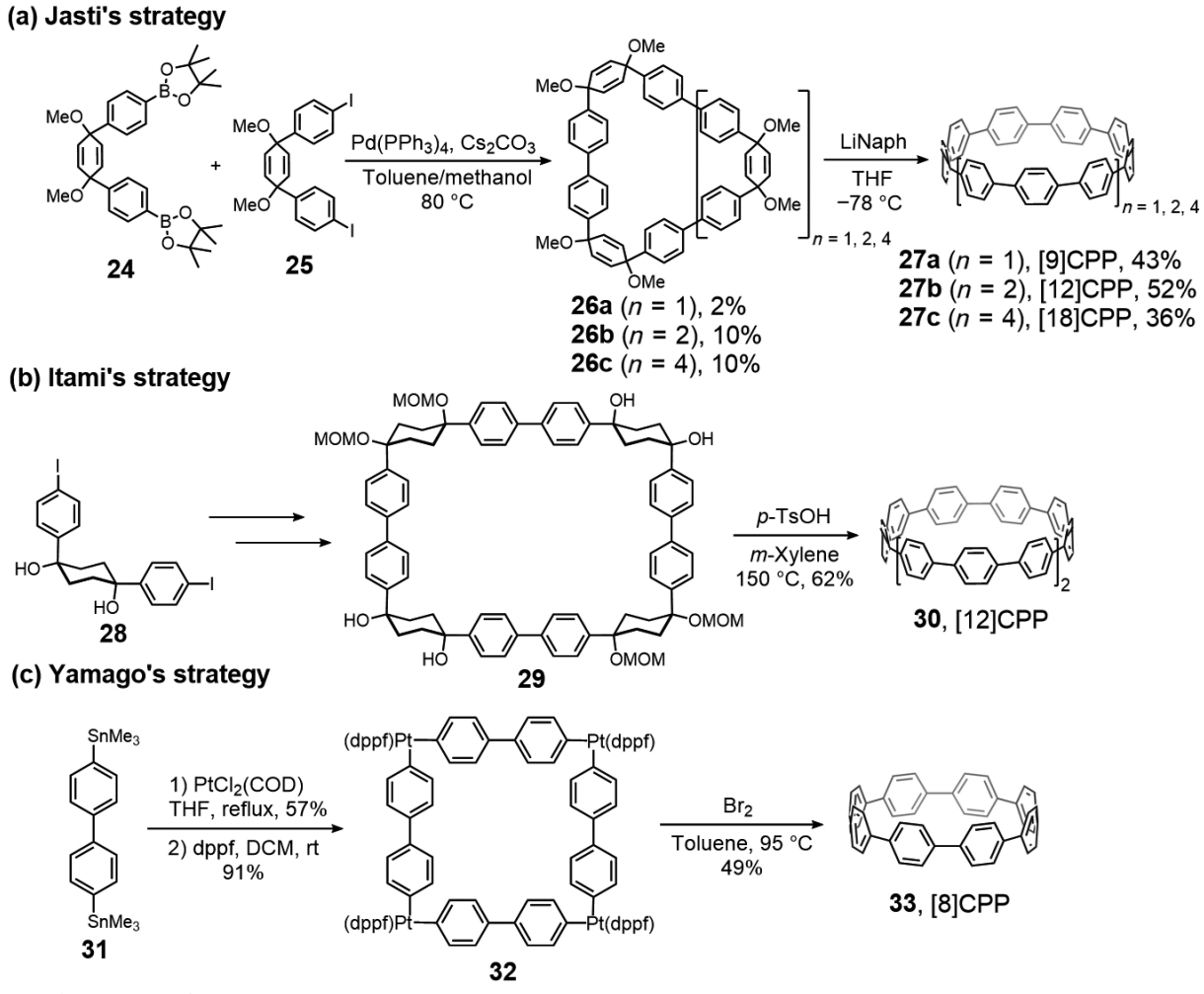

Figure 6 Synthetic strategies of CPPs.

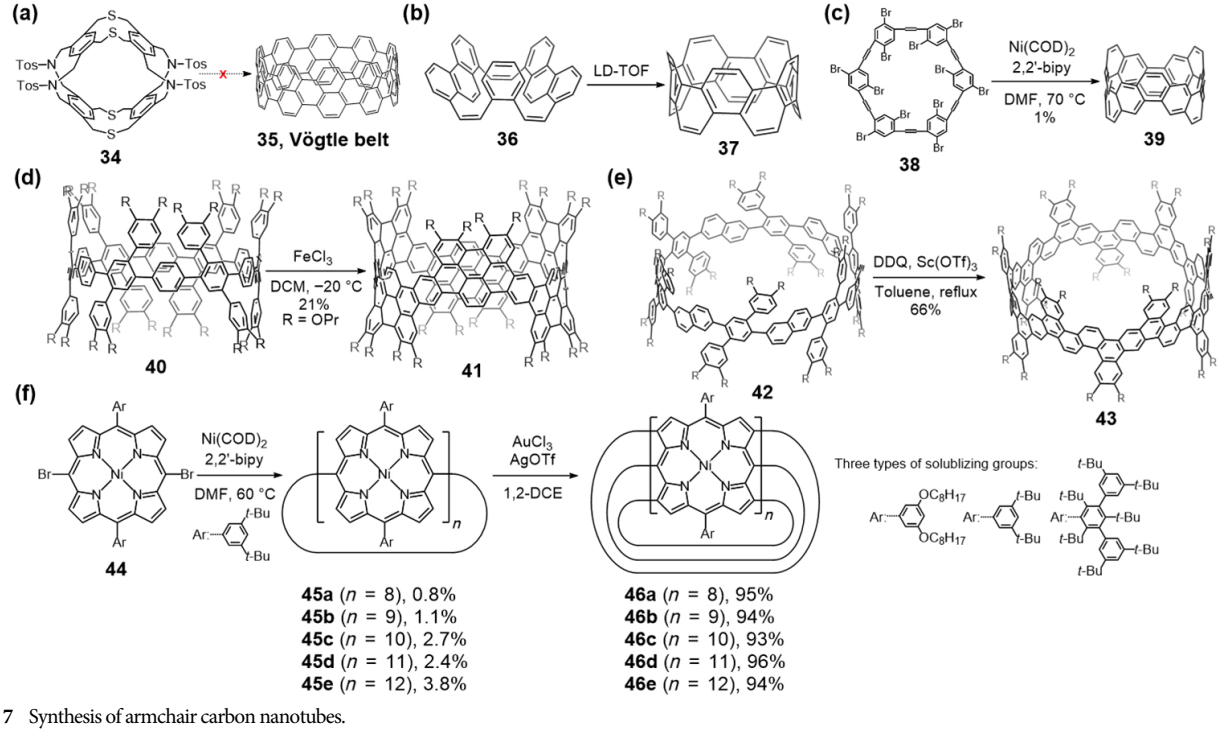

Figure 7 Synthesis of armchair carbon nanotubes.

effects, thereby facilitating the cyclization process. Recently, Anderson et al. synthesized porphyrin nanobelts **46** by nickel-mediated coupling ofmeso-bromoporphyrins to form singly linkednanorings, followed by oxidation with gold(III) chloride [68].

The synthesis of segments of zigzag carbon nanotubes, such as [*n*]cyclacenes or belt[*n*]arenes, can be expected to be more challenging due to their fully fused benzene ring structures forming a cyclic belt [69]. According to Clar's rule, extended linear annellation of benzene rings in one dimension significantly reduces the overall aromaticity [70]. Early attempts to synthesize [*n*]cyclacene via Diels–Alder reactions were hindered by aromatization in approaching the target molecules [71–73]. In 2016, Itami and colleagues attempted to obtain [12]cyclacene by cyclizing a macrocyclic precursor linked with alkynyl groups but observed an unexpected rearrangement instead [74]. It was not until 2020 when Wang and coworkers reported the observation of **51** using mass spectrometry (Fig. 8(a)) [75]. One year later, Itami et al. introduced an efficient strategy for synthesizing a derivative of [18]cyclacene **55** by constructing a macrocyclic precursor through a Diels–Alder reaction, followed by reduction using low-valent titanium (Fig. 8(b)) [76]. Around the same time, Chi et al. also reported the synthesis of a [12]cyclacene derivative **60** via a similar approach (Fig. 8(c)) [77]. In 2025, Chi et al. also synthesized non-alternant CNBs using an iterative Diels–Alder reaction followed by deoxygenative aromatization [78].

4 Carbon nanostructures with negative curvature

In the early 1890s, the mathematician Schwarz pioneered the study of triply periodic minimal surfaces (TPMS) and described several possible structures, such as the D-surface and the P-surface [4]. In 1991, Mackay and Terrones first proposed that carbon atoms could be arranged on these TPMS frameworks to form a novel three-dimensional carbon allotrope with negative curvature, which would require the incorporation of rings containing more than six carbon atoms [3]. The following year, in 1992, Elser and colleagues theoretically demonstrated an alternative approach to negatively curved graphite-like structures based on TPMS containing heptagonal and hexagonal rings [5]. They named this proposed carbon allotrope "schwarzite" in honor of the mathematician Schwarz.

The defining characteristic of schwarzites lies in the negative curvature of their atomic network. This structure is composed entirely of sp^2-hybridized carbon atoms, where the introduction of

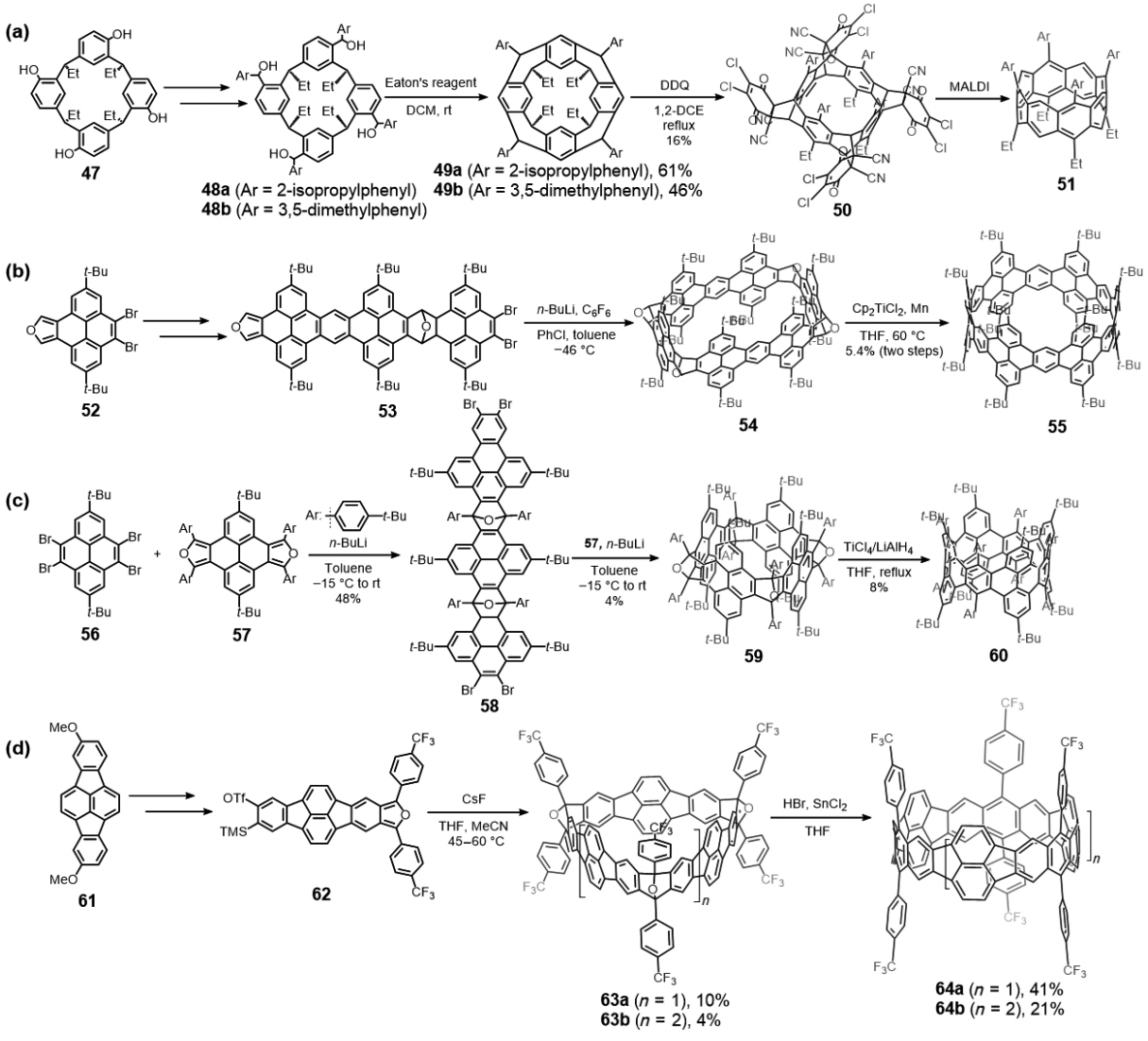

Figure 8 Synthesis of zigzag carbon nanotubes.

topological defects such as heptagons or octagons induces curvature into graphene-like sheets, forming a penetrating three-dimensional pore system. Based on their underlying geometric topology, they are primarily classified into families such as primitive-type (P), diamond-type (D), and gyroid-type (G). Taking the P192 structure as an example, its nomenclature directly reflects the primitive surface type and the unit cell composition of 192 carbon atoms. The structure can be described as an atomically precise "carbon nanofoam": a distorted sp^2 carbon network woven according to the strict topology of the P-surface, forming a periodic open framework with cubic symmetry and continuous channels. The P192 model elucidates, from the atomic scale, how the precise control over the type, quantity, and spatial distribution of non-hexagonal rings enables the construction of a macroscopically ordered carbon network with negative curvature. This provides a crucial theoretical blueprint for the "bottom-up" synthesis of such materials.

Schwarzites are characterized by highly symmetric structures and intricate interconnected cavities, endowing them with extremely high specific surface areas, exceptional mechanical strength, and other intriguing properties. Although schwarzites have not yet been synthesized to date, many theoretical studies suggest that this porous carbon-based nanomaterial holds promising potential for applications in energy storage systems due to their ultrahigh surface area and tunable pore architecture, enabling superior gas adsorption and electrochemical performance. Their unique negative curvature and electronic structure make them promising candidates for advanced catalysis and quantum computing applications. Additionally, the mechanically robust yet lightweight framework positions schwarzites as ideal materials for next-generation composite materials [6–10, 79].

A variety of synthesis methods for schwarzites have been proposed over the past few decades. In 2002, Milani et al. reported a sponge-like nanocarbon structure produced by bombarding graphite with a pulsed plasma cluster source under extremely low concentrations of organometallic catalysts [80]. Another idea is that template-mediated synthetic method may be of high efficiency to realize its precise synthesis. The resulting porous material exhibited structural features of negative curvature, drawing parallels to zeolites due to its porous nature [81, 82]. This similarity led to the hypothesis that zeolites could act as solid-phase templates for synthesizing schwarzite-like carbon. The proposed pathway involves the pyrolysis and reorganization of hydrocarbons on the zeolite surface, followed by template removal, to theoretically generate triply periodic carbon structures. The complex amorphous nature of these products presents significant challenges for precise characterization. In 2016, Ryoo and colleagues reported a 3D graphene-like structure that could be selectively constructed within zeolite templates, representing the carbon nanostructure most similar to schwarzites achieved to date [83]. Two years later, Smit and coworkers developed a theoretical framework through computational simulations that established a relationship between zeolite-templated carbons (ZTCs) and schwarzites, and identified specific zeolite types promising for the production of schwarzites via this method [81]. Simulation results indicated that P-type schwarzites, due to their higher strength and relatively greater thermodynamic stability, are likely the most promising candidate structures for experimental synthesis [79]. However, because of the lack of suitable templates and the limitations of current techniques, this zeolite-templating approach typically yields amorphous mixtures or non-periodic carbon materials, preventing the ZTC method from producing well-defined and macroscopically ordered schwarzites. A feasible strategy would be to synthesize molecular fragments exhibiting structural features of schwarzites first, and then use the fragments as seeds for the growth of macroscopically ordered schwarzites carbon [84–86].

From a structural perspective, the key feature of schwarzites is the incorporation of seven- or eight-membered rings, which introduce negative curvature and significant strain energy. Therefore, the synthesis of molecular carbons containing seven- or eight-membered rings is a critical initial step in the bottom-up construction of schwarzites. These negatively-curved molecular carbons, which inherently exhibit negative curvature, can serve not only as synthetic building blocks but also as model compounds for studying the influence of negatively curved topology on the properties of negatively-curved molecular carbons.

The synthesis of negatively-curved molecular carbons dates back to 1983, when Yamamoto et al. reported the synthesis and characterization of [7]circulene **65** via a two-step route involving photocyclization and McMurry coupling (Fig. 9(a)) [87]. [7]circulene can be regarded as the smallest fragment representing the structural features of schwarzite P216. Due to the synthetic challenges, Suzuki and Sakamoto, and the group of Wu independently reported the synthesis of [8]circulene and tetrabenzo[8]circulene respectively until 2013, which is the smallest fragment embodying the structural characteristics of schwarzite P192 [88, 89]. Suzuki and Sakamoto adopted an "out–in" strategy, constructing a cyclic octaphenylene precursor via palladium-catalyzed cross-coupling, followed by a Scholl reaction to form the highly strained eight-membered ring, yielding tetrabenzo[8]circulene **69** (Fig. 9(e)). In contrast, Wu et al. employed a fundamentally different approach, first building the central eight-membered ring and then performing a palladium-catalyzed cyclization using symmetrically substituted diarylacetylenes and iodinated precursors to afford [8]circulene. Single-crystal X-ray diffraction confirmed a deep saddle-shaped geometry resulting from the presence of the octagonal ring. The synthesis of [7]circulene and [8]circulene significantly advanced the field of negatively curved PAHs and inspired the pursuit of schwarzite fragments containing multiple non-hexagonal rings. Besides, Itami et al. also reported the synthesis of a grossly warped nanographenes that contains one 5-membered ring and five 7-membered rings by oxidation reaction [90]. Although not fitting into a classical schwarzite structure, this C_{80} molecule carbon exhibits significant negative curvature characteristics. In 2015, Miao et al. reported the synthesis of a saddle-shaped PAH containing two heptagonal rings via an oxidative cyclodehydrogenation with 2,3-dicyano-5,6-dichlorobenzoquinone (DDQ) [91]. This molecule can be viewed as a fragment of schwarzite P216. Two years later, Miao et al. described the synthesis of dipleiadiene, an SR-PAH **66** (Fig. 9(b)) with 46 carbon atoms, which constitutes a substructure of schwarzite D216 [92]. In 2019, Würthner et al. developed a palladium-catalyzed [5+2] cyclization strategy for the rational synthesis of negatively curved heptagon-containing PAHs [93]. In 2024, Mastalerz et al. reported aromatic saddle-shaped PAHs **67**, which represent extensive substructures of schwarzite P216 [94] (Fig. 9(c)). The symmetric incorporation of four heptagonal rings leads to pronounced bending of the entire backbone, generating two saddle-shaped surfaces. The largest saddle surface measures 11.2 Å in width and 4.64 Å in depth. In 2025, Miao's group

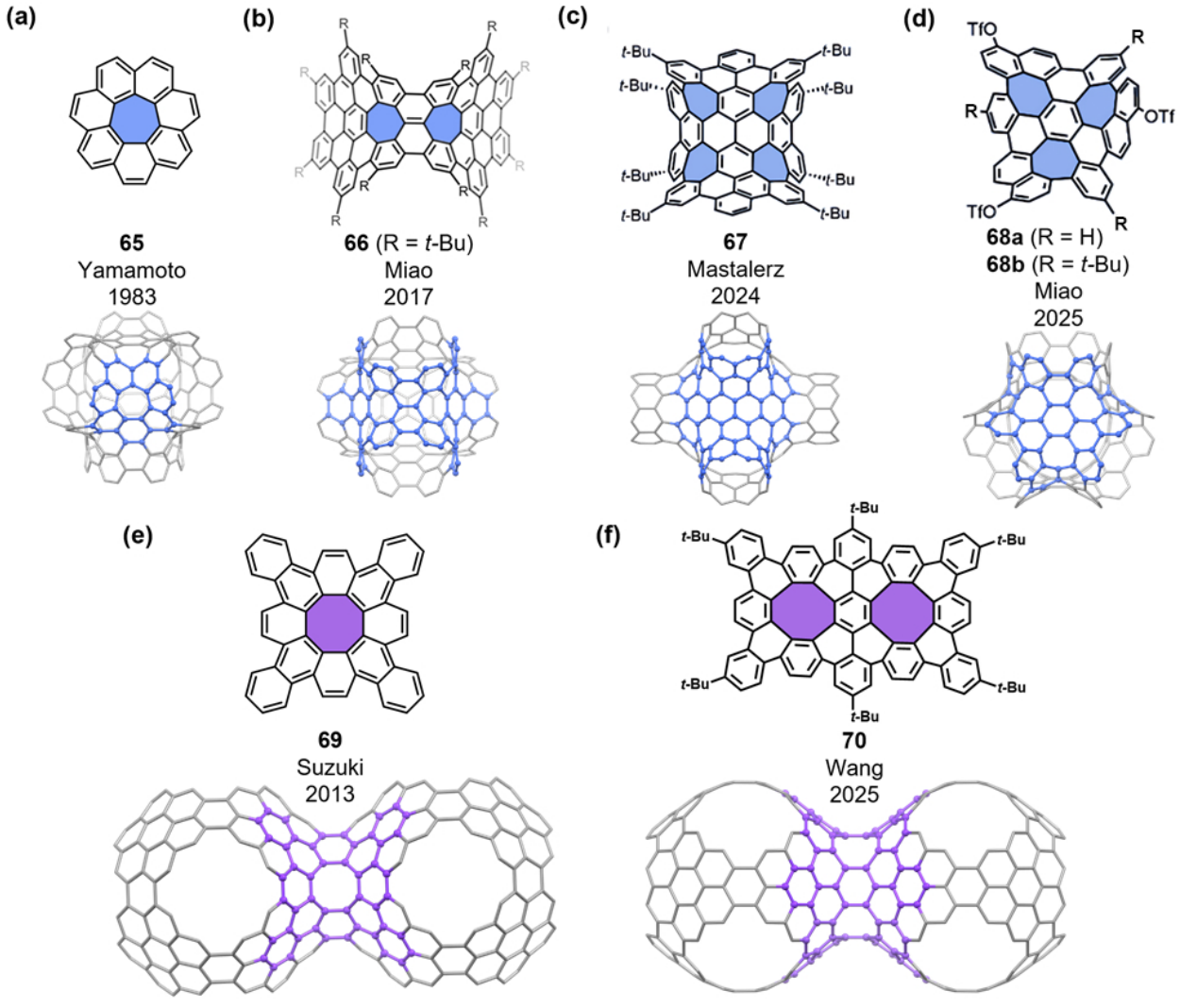

Figure 9 Negatively-curved molecular carbons.

reported another key fragment **68** of schwarzite P216 containing three heptagonal rings [95]. The C_3-symmetric point group endows it with a characteristic "monkey saddle" configuration (Fig. 9(d)). Most recently, our group reported the synthesis of a semi-tubular aromatic fragment **70** of schwarzite P192 containing two octagonal rings (Fig. 9(f)) [96]. This C_{78} fragment is the largest known SR-PAH to date, accounting for 41% of the P192 unit cell volume. In this molecular carbon, each of the two octagonal rings induces a bending of approximately 90° in the same direction, resulting in a nearly 180° curvature of the conjugated molecular backbone. The root-mean-square deviation between its molecular structure and the corresponding fragment in schwarzite P192 is only 0.37 Å, indicating that the highly distorted carbon structure in schwarzite P192 is intrinsically consistent with the configuration of such negatively curved molecular carbons. This provides a fundamental basis for synthesizing the key negatively curved structural units required for schwarzite P192.

5 Conclusions

Curved carbon nanomaterials constitute a significant class of materials due to their unique geometric structures and corresponding physicochemical properties, which underpin broad potential applications. Despite the availability of conventional synthesis routes, the precise and controllable fabrication of these materials remains both critically important and challenging. In recent decades, bottom-up synthetic strategies have emerged as a powerful approach, offering distinct advantages for advancing this field. First, molecular carbon nanostructures derived from the extension of polycyclic aromatic hydrocarbons represent atomically precise entities. Their well-defined structures serve as ideal prototypes for establishing unambiguous structure–property relationships. Second, the chemical synthesis of such molecular carbons provides a versatile platform for accessing a diverse range of nanostructures. Furthermore, they serve as a programmable molecular platform for building larger carbon architectures by enabling controlled assembly or transformation.

Therefore, future research should prioritize the following key directions to address existing challenges and harness emerging opportunities: (1) Advancing atomically precise synthesis. The comprehensive and simultaneous control over multiple structural parameters (e.g., chirality, diameter, length, and edge topology) remains a paramount challenge. While methods like chemical vapor deposition have achieved chirality-specific growth of carbon nanotubes, synergistic control over other dimensions is still limited. Developing synthetic methodologies with enhanced selectivity and

scalability is essential for moving from singular parameter control to integrated multidimensional design. (2) Elucidating structure–property relationships for targeted applications. A deeper understanding requires the integration of advanced *in situ* characterization with multiscale computational simulations. This correlation is crucial for unraveling how curvature and topology dictate optical, electronic, and catalytic behaviors. Research should focus on properties arising from curvature to guide application-driven development in energy, electronics, and sensing technologies. (3) Extending from molecular to infinite system. How to realize the precise synthesis of Schwarzite carbons has become the most intriguing scientific holy grail. Realizing this "molecular building-block" approach necessitates innovative coupling and assembly strategies, demanding close collaboration between organic chemists, materials scientists, and theoreticians.

By continuously focusing on these fields, research on curved carbon nanomaterials holds promise for not only uncovering new physical properties of carbon materials but also providing innovative material solutions for next-generation energy, electronics, and quantum technologies.

Data availability

Not applicable.

Acknowledgements

This work was financially supported by the National Natural Science Foundation of China (NSFC) (No. 22350005).

Declaration of competing interest

All the contributing authors report no conflict of interests in this work.

Author contribution statement

Q. R. L.: Writing – original draft, writing – review & editing. M.-W. W.: Writing – review & editing, supervision. W. J.: Project administration, supervison. Z. H. W.: Project administration, funding acquisition, supervision.

Use of AI statement

None.

References

[1] Kroto, H. W.; Heath, J. R.; O'Brien, S. C.; Curl, R. F.; Smalley, R. E. C_{60}: Buckminsterfullerene. *Nature* **1985**, *318*, 162–163.
[2] Iijima, S. Helical microtubules of graphitic carbon. *Nature* **1991**, *354*, 56–58.
[3] Mackay, A. L.; Terrones, H. Diamond from graphite. *Nature* **1991**, *352*, 762.
[4] Schwarz, H. A. *Gesammelte Mathematische Abhandlungen*; Springer: Berlin, 1890.
[5] Lenosky, T.; Gonze, X.; Teter, M.; Elser, V. Energetics of negatively curved graphitic carbon. *Nature* **1992**, *355*, 333–335.
[6] Park, N.; Yoon, M.; Berber, S.; Ihm, J.; Osawa, E.; Tománek, D. Magnetism in all-carbon nanostructures with negative Gaussian curvature. *Phys. Rev. Lett.* **2003**, *91*, 237204.
[7] Ruoff, R. S. Personal perspectives on graphene: New graphene-related materials on the horizon. *MRS Bull.* **2012**, *37*, 1314–1318.
[8] Odkhuu, D.; Jung, D. H.; Lee, H.; Han, S. S.; Choi, S. H.; Ruoff, R. S.; Park, N. Negatively curved carbon as the anode for lithium ion batteries. *Carbon* **2014**, *66*, 39–47.
[9] Borges, D. D.; Galvao, D. S. Schwarzites for natural gas storage: A grand-canonical Monte Carlo study. *MRS Adv.* **2018**, *3*, 115–120.
[10] Krasnov, P. O.; Shkaberina, G. S.; Polyutov, S. P. Molecular hydrogen sorption capacity of *P*216-schwarzite: PM6-D3, MP2 and QTAIM approaches. *Comput. Mater. Sci.* **2022**, *209*, 111410.
[11] Krätschmer, W.; Lamb, L. D.; Fostiropoulos, K.; Huffman, D. R. Solid C_{60}: A new form of carbon. *Nature* **1990**, *347*, 354–358.
[12] Parker, D. H.; Wurz, P.; Chatterjee, K.; Lykke, K. R.; Hunt, J. E.; Pellin, M. J.; Hemminger, J. C.; Gruen, D. M.; Stock, L. M. High-yield synthesis, separation, and mass-spectrometric characterization of fullerenes C_{60} to C_{266}. *J. Am. Chem. Soc.* **1991**, *113*, 7499–7503.
[13] Segawa, Y.; Levine, D. R.; Itami, K. Topologically unique molecular nanocarbons. *Acc. Chem. Res.* **2019**, *52*, 2760–2767.
[14] Li, C. Z.; Yip, H. L.; Jen, A. K. Y. Functional fullerenes for organic photovoltaics. *J. Mater. Chem.* **2012**, *22*, 4161–4177.
[15] Dugan, L. L.; Lovett, E. G.; Quick, K. L.; Lotharius, J.; Lin, T. T.; O'Malley, K. L. Fullerene-based antioxidants and neurodegenerative disorders. *Parkinsonism Relat. Disord.* **2001**, *7*, 243–246.
[16] Sarkar, M.; Santra, D. Fullerene based materials for drug delivery. In *Carbon Based Nanomaterials for Drug Delivery*. Swain, S. K., Ed.; Springer: Singapore, 2025; pp 323–355.
[17] Zhang, Y. Y.; Peng, X. B.; Tian, H. R.; Yang, B.; Chen, Z. C.; Li, J. J.; Zhang, T. H.; Zhang, M. Y.; Liang, X. C.; Yu, Z. Y. et al. Fullerene on non-iron cluster-matrix co-catalysts promotes collaborative H_2 and N_2 activation for ammonia synthesis. *Nat. Chem.* **2024**, *16*, 1781–1787.
[18] Gravel, E.; Doris, E. Fullerenes make copper catalysis better. *Science* **2022**, *376*, 242–243.
[19] McElvany, S. W.; Ross, M. M.; Goroff, N. S.; Diederich, F. Cyclocarbon coalescence: Mechanisms for tailor-made fullerene formation. *Science* **1993**, *259*, 1594–1596.
[20] Rubin, Y.; Parker, T. C.; Khan, S. I.; Holliman, C. L.; McElvany, S. W. Precursors to endohedral metal fullerene complexes: Synthesis and X-ray structure of a flexible acetylenic cyclophane $C_{60}H_{18}$. *J. Am. Chem. Soc.* **1996**, *118*, 5308–5309.
[21] Tobe, Y.; Nakagawa, N.; Naemura, K.; Wakabayashi, T.; Shida, T.; Achiba, Y. [16.16.16](1,3,5)Cyclophanetetracosayne ($C_{60}H_6$): A precursor to C_{60} fullerene. *J. Am. Chem. Soc.* **1998**, *120*, 4544–4545.
[22] Bunz, U. H. F.; Rubin, Y.; Tobe, Y. Polyethynylated cyclic π-systems: Scaffoldings for novel two and three-dimensional carbon networks. *Chem. Soc. Rev.* **1999**, *28*, 107–119.
[23] Scott, L. T.; Hashemi, M. M.; Bratcher, M. S. Corannulene bowl-to-bowl inversion is rapid at room temperature. *J. Am. Chem. Soc.* **1992**, *114*, 1920–1921.
[24] Borchardt, A.; Fuchicello, A.; Kilway, K. V.; Baldridge, K. K.; Siegel, J. S. Synthesis and dynamics of the corannulene nucleus. *J. Am. Chem. Soc.* **1992**, *114*, 1921–1923.
[25] Rabideau, P. W.; Abdourazak, A. H.; Folsom, H. E.; Marcinow, Z.; Sygula, A.; Sygula, R. Buckybowls: Synthesis and *ab initio* calculated structure of the first semibuckminsterfullerene. *J. Am. Chem. Soc.* **1994**, *116*, 7891–7892.
[26] Hagen, S.; Bratcher, M. S.; Erickson, M. S.; Zimmermann, G.; Scott, L. T. Novel syntheses of three $C_{30}H_{12}$ bowl-shaped polycyclic aromatic hydrocarbons. *Angew. Chem., Int. Ed.* **1997**, *36*, 406–408.
[27] Abdourazak, A. H.; Sygula, A.; Rabideau, P. W. "Locking" the bowl-shaped geometry of corannulene: Cyclopentacorannulene. *J. Am. Chem. Soc.* **1993**, *115*, 3010–3011.
[28] Ansems, R. B. M.; Scott, L. T. Circumtrindene: A geodesic dome of molecular dimensions. Rational synthesis of 60 of C_{60}[1]. *J. Am. Chem. Soc.* **2000**, *122*, 2719–2724.
[29] Scott, L. T.; Bratcher, M. S.; Hagen, S. Synthesis and characterization of a $C_{36}H_{12}$ fullerene subunit. *J. Am. Chem. Soc.* **1996**, *118*, 8743–8744.

[30] Abdourazak, A. H.; Marcinow, Z.; Sygula, A.; Sygula, R.; Rabideau, P. W. Buckybowls 2. Toward the total synthesis of buckminsterfullerene (C_{60}): Benz[5,6]-as-indaceno[3,2,1,8,7-mnopqr]indeno[4,3,2,1-cdef]chrysene. *J. Am. Chem. Soc.* **1995**, *117*, 6410–6411.

[31] Forkey, D. M.; Attar, S.; Noll, B. C.; Koerner, R.; Olmstead, M. M.; Balch, A. L. Crystallographic characterization of the molecular structure and solid state packing of the fullerene-shaped hydrocarbon $C_{36}H_{12}$. *J. Am. Chem. Soc.* **1997**, *119*, 5766–5767.

[32] Boorum, M. M.; Vasil'ev, Y. V.; Drewello, T.; Scott, L. T. Groundwork for a rational synthesis of C_{60}: Cyclodehydrogenation of a $C_{60}H_{30}$ polyarene. *Science* **2001**, *294*, 828–831.

[33] Scott, L. T.; Boorum, M. M.; McMahon, B. J.; Hagen, S.; Mack, J.; Blank, J.; Wegner, H.; de Meijere, A. A rational chemical synthesis of C_{60}. *Science* **2002**, *295*, 1500–1503.

[34] Majewski, M. A.; Stępień, M. Bowls, hoops, and saddles: Synthetic approaches to curved aromatic molecules. *Angew. Chem., Int. Ed.* **2019**, *58*, 86–116.

[35] Amaya, T.; Seki, S.; Moriuchi, T.; Nakamoto, K.; Nakata, T.; Sakane, H.; Saeki, A.; Tagawa, S.; Hirao, T. Anisotropic electron transport properties in sumanene crystal. *J. Am. Chem. Soc.* **2009**, *131*, 408–409.

[36] Jackson, E. A.; Steinberg, B. D.; Bancu, M.; Wakamiya, A.; Scott, L. T. Pentaindenocorannulene and tetraindenocorannulene: New aromatic hydrocarbon π systems with curvatures surpassing that of C_{60}. *J. Am. Chem. Soc.* **2007**, *129*, 484–485.

[37] Otero, G.; Biddau, G.; Sánchez-Sánchez, C.; Caillard, R.; López, M. F.; Rogero, C.; Palomares, F. J.; Cabello, N.; Basanta, M. A.; Ortega, J. et al. Fullerenes from aromatic precursors by surface-catalysed cyclodehydrogenation. *Nature* **2008**, *454*, 865–868.

[38] Iijima, S.; Ichihashi, T. Single-shell carbon nanotubes of 1-nm diameter. *Nature* **1993**, *363*, 603–605.

[39] Bethune, D. S.; Kiang, C. H.; de Vries, M. S.; Gorman, G.; Savoy, R.; Vazquez, J.; Beyers, R. Cobalt-catalysed growth of carbon nanotubes with single-atomic-layer walls. *Nature* **1993**, *363*, 605–607.

[40] Dai, H. J. Carbon nanotubes: Synthesis, integration, and properties. *Acc. Chem. Res.* **2002**, *35*, 1035–1044.

[41] De Volder, M. F. L.; Tawfick, S. H.; Baughman, R. H.; Hart, A. J. Carbon nanotubes: Present and future commercial applications. *Science* **2013**, *339*, 535–539.

[42] Yu, L. P.; Shearer, C.; Shapter, J. Recent development of carbon nanotube transparent conductive films. *Chem. Rev.* **2016**, *116*, 13413–13453.

[43] Zhang, R. F.; Zhang, Y. Y.; Wei, F. Horizontally aligned carbon nanotube arrays: Growth mechanism, controlled synthesis, characterization, properties and applications. *Chem. Soc. Rev.* **2017**, *46*, 3661–3715.

[44] Liu, B. L.; Wu, F. Q.; Gui, H.; Zheng, M.; Zhou, C. W. Chirality-controlled synthesis and applications of single-wall carbon nanotubes. *ACS Nano* **2017**, *11*, 31–53.

[45] Bachilo, S. M.; Balzano, L.; Herrera, J. E.; Pompeo, F.; Resasco, D. E.; Weisman, R. B. Narrow (*n,m*)-distribution of single-walled carbon nanotubes grown using a solid supported catalyst. *J. Am. Chem. Soc.* **2003**, *125*, 11186–11187.

[46] Zhu, H. W.; Suenaga, K.; Hashimoto, A.; Urita, K.; Hata, K.; Iijima, S. Atomic-resolution imaging of the nucleation points of single-walled carbon nanotubes. *Small* **2005**, *1*, 1180–1183.

[47] Reich, S.; Li, L.; Robertson, J. Control the chirality of carbon nanotubes by epitaxial growth. *Chem. Phys. Lett.* **2006**, *421*, 469–472.

[48] Harutyunyan, A. R.; Chen, G. G.; Paronyan, T. M.; Pigos, E. M.; Kuznetsov, O. A.; Hewaparakrama, K.; Kim, S. M.; Zakharov, D.; Stach, E. A.; Sumanasekera, G. U. Preferential growth of single-walled carbon nanotubes with metallic conductivity. *Science* **2009**, *326*, 116–120.

[49] Zhang, S. C.; Kang, L. X.; Wang, X.; Tong, L. M.; Yang, L. W.; Wang, Z. Q.; Qi, K.; Deng, S. B.; Li, Q. W.; Bai, X. D. et al. Arrays of horizontal carbon nanotubes of controlled chirality grown using designed catalysts. *Nature* **2017**, *543*, 234–238.

[50] Yang, F.; Wang, X.; Zhang, D. Q.; Yang, J.; Luo, D.; Xu, Z. W.; Wei, J. K.; Wang, J. Q.; Xu, Z.; Peng, F. et al. Chirality-specific growth of single-walled carbon nanotubes on solid alloy catalysts. *Nature* **2014**, *510*, 522–524.

[51] Yang, F.; Wang, X.; Zhang, D. Q.; Qi, K.; Yang, J.; Xu, Z.; Li, M. H.; Zhao, X. L.; Bai, X. D.; Li, Y. Growing zigzag (16,0) carbon nanotubes with structure-defined catalysts. *J. Am. Chem. Soc.* **2015**, *137*, 8688–8691.

[52] Yang, F.; Wang, X.; Si, J.; Zhao, X. L.; Qi, K.; Jin, C. H.; Zhang, Z. Y.; Li, M. H.; Zhang, D. Q.; Yang, J. et al. Water-assisted preparation of high-purity semiconducting (14,4) carbon nanotubes. *ACS Nano* **2017**, *11*, 186–193.

[53] Zhao, X. L.; Yang, F.; Chen, J. H.; Ding, L.; Liu, X. Y.; Yao, F. R.; Li, M. H.; Zhang, D. Q.; Zhang, Z. Y.; Liu, X. et al. Selective growth of chirality-enriched semiconducting carbon nanotubes by using bimetallic catalysts from salt precursors. *Nanoscale* **2018**, *10*, 6922–6927.

[54] Scott, L. T.; Jackson, E. A.; Zhang, Q. Y.; Steinberg, B. D.; Bancu, M.; Li, B. A short, rigid, structurally pure carbon nanotube by stepwise chemical synthesis. *J. Am. Chem. Soc.* **2012**, *134*, 107–110.

[55] Omachi, H.; Nakayama, T.; Takahashi, E.; Segawa, Y.; Itami, K. Initiation of carbon nanotube growth by well-defined carbon nanorings. *Nat. Chem.* **2013**, *5*, 572–576.

[56] Sanchez-Valencia, J. R.; Dienel, T.; Gröning, O.; Shorubalko, I.; Mueller, A.; Jansen, M.; Amsharov, K.; Ruffieux, P.; Fasel, R. Controlled synthesis of single-chirality carbon nanotubes. *Nature* **2014**, *512*, 61–64.

[57] Liu, B. L.; Liu, J.; Li, H. B.; Bhola, R.; Jackson, E. A.; Scott, L. T.; Page, A.; Irle, S.; Morokuma, K.; Zhou, C. W. Nearly exclusive growth of small diameter semiconducting single-wall carbon nanotubes from organic chemistry synthetic end-cap molecules. *Nano Lett.* **2015**, *15*, 586–595.

[58] Jasti, R.; Bhattacharjee, J.; Neaton, J. B.; Bertozzi, C. R. Synthesis, characterization, and theory of [9]-, [12]-, and [18]cycloparaphenylene: Carbon nanohoop structures. *J. Am. Chem. Soc.* **2008**, *130*, 17646–17647.

[59] Takaba, H.; Omachi, H.; Yamamoto, Y.; Bouffard, J.; Itami, K. Selective synthesis of [12]cycloparaphenylene. *Angew. Chem., Int. Ed.* **2009**, *48*, 6112–6116.

[60] Yamago, S.; Watanabe, Y.; Iwamoto, T. Synthesis of [8]cycloparaphenylene from a square-shaped tetranuclear platinum complex. *Angew. Chem., Int. Ed.* **2010**, *49*, 757–759.

[61] Tsuchido, Y.; Abe, R.; Ide, T.; Osakada, K. A Macrocyclic gold(I)-biphenylene complex: Triangular molecular structure with twisted Au_2(diphosphine) corners and reductive elimination of [6]Cycloparaphenylene. *Angew. Chem., Int. Ed.* **2020**, *59*, 22928–22932.

[62] Guo, Q. H.; Qiu, Y. Y.; Wang, M. X.; Fraser Stoddart, J. Aromatic hydrocarbon belts. *Nat. Chem.* **2021**, *13*, 402–419.

[63] Vögtle, F.; Schröder, A.; Karbach, D. Strategy for the synthesis of tube-shaped molecules. *Angew. Chem., Int. Ed.* **1991**, *30*, 575–577.

[64] Iyoda, M.; Kuwatani, Y.; Nishinaga, T.; Takase, M.; Nishiuchi, T. Conjugated molecular belts based on 3D benzannulene systems. In *Fragments of Fullerenes and Carbon Nanotubes: Designed Synthesis, Unusual Reactions, and Coordination Chemistry*. Petrukhina, M. A.; Scott, L. T., Eds.; Wiley: Hoboken, 2012; pp 311–342.

[65] Povie, G.; Segawa, Y.; Nishihara, T.; Miyauchi, Y.; Itami, K. Synthesis of a carbon nanobelt. *Science* **2017**, *356*, 172–175.

[66] Povie, G.; Segawa, Y.; Nishihara, T.; Miyauchi, Y.; Itami, K. Synthesis and size-dependent properties of [12], [16], and [24]carbon nanobelts. *J. Am. Chem. Soc.* **2018**, *140*, 10054–10059.

[67] Cheung, K. Y.; Gui, S. J.; Deng, C. F.; Liang, H. F.; Xia, Z. M.; Liu, Z. F.; Chi, L. F.; Miao, Q. Synthesis of armchair and chiral carbon nanobelts. *Chem* **2019**, *5*, 838–847.

[68] Rodríguez-Rubio, A.; Zhu, H.; Man Cheung, K.; Rončević, I.; Gödde, L. A.; Hergenhahn, J.; Field, J. L.; Gupta, P.; Stawski, W.; Gotfredsen, H. et al. Synthesis of triple stranded porphyrin nanobelts. *Science* **2025**, *390*, 290–293.
[69] Heilbronner, E. Molecular orbitals in homologen reihen mehrkerniger aromatischer kohlenwasserstoffe: I. Die eigenwerte yon LCAO-MO's in homologen reihen. *Helv. Chim. Acta* **1954**, *37*, 921–935.
[70] Clar, E. *The Aromatic Sextet*; Wiley: New York, 1972.
[71] Kohnke, F. H.; Slawin, A. M. Z.; Stoddart, J. F.; Williams, D. J. Molecular belts and collars in the making: A hexaepoxyoctacosahydro[12]cyclacene derivative. *Angew. Chem., Int. Ed.* **1987**, *26*, 892–894.
[72] Cory, R. M.; McPhail, C. L.; Dikmans, A. J.; Vittal, J. J. Macrocyclic cyclophane belts via double Diels–Alder cycloadditions: Macroannulation of bisdienes by bisdienophiles. Synthesis of a key precursor to an [8]cyclacene. *Tetrahedron Lett.* **1996**, *37*, 1983–1986.
[73] Cory, R. M.; McPhail, C. L. Transformations of a macrocyclic cyclophane belt into advanced [8]cyclacene and [8]cyclacene triquinone precursors. *Tetrahedron Lett.* **1996**, *37*, 1987–1990.
[74] Matsui, K.; Fushimi, M.; Segawa, Y.; Itami, K. Synthesis, structure, and reactivity of a cylinder-shaped cyclo[12]orthophenylene[6]ethynylene: Toward the synthesis of zigzag carbon nanobelts. *Org. Lett.* **2016**, *18*, 5352–5355.
[75] Shi, T. H.; Guo, Q. H.; Tong, S.; Wang, M. X. Toward the synthesis of a highly strained hydrocarbon belt. *J. Am. Chem. Soc.* **2020**, *142*, 4576–4580.
[76] Cheung, K. Y.; Watanabe, K.; Segawa, Y.; Itami, K. Synthesis of a zigzag carbon nanobelt. *Nat. Chem.* **2021**, *13*, 255–259.
[77] Han, Y.; Dong, S. Q.; Shao, J. W.; Fan, W.; Chi, C. Y. Synthesis of a sidewall fragment of a (12,0) carbon nanotube. *Angew. Chem., Int. Ed.* **2021**, *60*, 2658–2662.
[78] Han, Y.; Wu, S. F.; Khoo, K. Y. S.; Chi, C. Y. Synthesis of fully π-conjugated non-alternant carbon nanobelts. *Nat. Synth.* **2025**, *4*, 947–955.
[79] Miller, D. C.; Terrones, M.; Terrones, H. Mechanical properties of hypothetical graphene foams: Giant schwarzites. *Carbon* **2016**, *96*, 1191–1199.
[80] Barborini, E.; Piseri, P.; Milani, P.; Benedek, G.; Ducati, C.; Robertson, J. Negatively curved spongy carbon. *Appl. Phys. Lett.* **2002**, *81*, 3359–3361.
[81] Braun, E.; Lee, Y.; Moosavi, S. M.; Barthel, S.; Mercado, R.; Baburin, I. A.; Proserpio, D. M.; Smit, B. Generating carbon schwarzites via zeolite-templating. *Proc. Natl. Acad. Sci. USA* **2018**, *115*, E8116–E8124.
[82] Taylor, E. E.; Garman, K.; Stadie, N. P. Atomistic structures of zeolite-templated carbon. *Chem. Mater.* **2020**, *32*, 2742–2752.
[83] Kim, K.; Lee, T.; Kwon, Y.; Seo, Y.; Song, J.; Park, J. K.; Lee, H.; Park, J. Y.; Ihee, H.; Cho, S. J. et al. Lanthanum-catalysed synthesis of microporous 3D graphene-like carbons in a zeolite template. *Nature* **2016**, *535*, 131–135.
[84] Pun, S. H.; Miao, Q. Toward negatively curved carbons. *Acc. Chem. Res.* **2018**, *51*, 1630–1642.
[85] Segawa, Y.; Ito, H.; Itami, K. Structurally uniform and atomically precise carbon nanostructures. *Nat. Rev. Mater.* **2016**, *1*, 15002.
[86] Wang, M. W.; Fan, W.; Li, X. N.; Liu, Y. J.; Li, Z. Y.; Jiang, W.; Wu, J. S.; Wang, Z. H. Molecular carbons: How far can we go. *ACS Nano* **2023**, *17*, 20734–20752.
[87] Yamamoto, K.; Harada, T.; Nakazaki, M.; Naka, T.; Kai, Y.; Harada, S.; Kasai, N. Synthesis and characterization of [7]circulene. *J. Am. Chem. Soc.* **1983**, *105*, 7171–7172.
[88] Sakamoto, Y.; Suzuki, T. Tetrabenzo[8]circulene: Aromatic saddles from negatively curved graphene. *J. Am. Chem. Soc.* **2013**, *135*, 14074–14077.
[89] Feng, C. N.; Kuo, M. Y.; Wu, Y. T. Synthesis, structural analysis, and properties of [8]circulenes. *Angew. Chem., Int. Ed.* **2013**, *52*, 7791–7794.
[90] Kawasumi, K.; Zhang, Q. Y.; Segawa, Y.; Scott, L. T.; Itami, K. A grossly warped nanographene and the consequences of multiple odd-membered-ring defects. *Nat. Chem.* **2013**, *5*, 739–744.
[91] Cheung, K. Y.; Xu, X. M.; Miao, Q. Aromatic saddles containingtwoheptagons. *J. Am. Chem. Soc.* **2015**, *137*, 3910–3914.
[92] Cheung, K. Y.; Chan, C. K.; Liu, Z. F.; Miao, Q. A twisted nanographene consisting of 96 carbon atoms. *Angew. Chem., Int. Ed.* **2017**, *56*, 9003–9007.
[93] Farrell, J. M.; Grande, V.; Schmidt, D.; Würthner, F. A highly warped heptagon-containing sp^2 carbon scaffold via vinylnaphthyl π-extension. *Angew. Chem., Int. Ed.* **2019**, *58*, 16504–16507.
[94] Elbert, S. M.; Paine, O. T. A.; Kirschbaum, T.; Schuldt, M. P.; Weber, L.; Rominger, F.; Mastalerz, M. A negatively curved nanographene with four embedded heptagons. *J. Am. Chem. Soc.* **2024**, *146*, 27324–27334.
[95] Yang, X. H.; Su, S. L.; Hu, C. Y.; Cheung, K. M.; Yang, D. Y.; Chen, X.; Yang, J.; Huang, Z. F.; Kwong, F. Y.; Miao, Q. A key fragment in carbon schwarzite unit cells and its triple [6]helicene precursor. *Angew. Chem., Int. Ed.* **2025**, *64*, e202501169.
[96] Wang, M. W.; Chan, J.; Long, Q. R.; Wagenhäuser, Y.; Würthner, F.; Jiang, W.; Wang, Z. H. Semitubular aromatic fragment of schwarzite P192: A conserved structural motif with two embedded octagons. *J. Am. Chem. Soc.* **2025**, *147*, 47102–47108.